SUPPLEMENTAL MATERIALS

Material and Methods

Monitoring and analysis of tumor burdened mice. Experimental mice were monitored with assistance from professional animal technicians on a three-times per week basis routinely and daily if any concerns developed regarding their wellbeing. Signs of illness include respiratory distress, weight loss, hunched posture, slow movement, hind leg paralysis and enlarged lymph nodes and/or spleen. If signs of illness developed, the mice were euthanized using CO_2 asphyxiation. Euthanized mice were examined, peripheral blood samples were obtained using retro-orbital venesection and organs collected for histological analysis included thymus, spleen, lymph node, kidney, liver, sternum, heart, lung and vertebrae. All organs were preserved in 10% buffered formalin. Blood analysis was performed using the ADVIA automated hemocytometer (Bayer, Tarrytown, NY, USA). Organ cellularity was determined by measuring cell counts on a single cell suspension obtained from a whole organ in a known volume of tissue culture medium. Cell counts were determined using the Scharfe System CASY counter. For flow cytometric analysis, a single cell suspension of the tissue of interest was prepared using a 100 μm cell strainer (Falcon #352360). Tumor immuno-phenotyping was performed on aliquots of cells by flow cytometric analysis.

Quantitative PCR assay for *Trp53* genomic DNA copy number and *Trp53* exon sequencing. Primer sets were ordered for "Primetime qPCR Assay" from Integrated DNA Technologies (IDT). Assay design was carried out using the primer quest tool (IDT). Sequences were as follows: Exon 4 for: 5'- GGTTCTTCTTTGTCCCATCC and rev: 5'- CTTCACTTGGGCCTTCAAA and probe target sequence: 5'-56-FAM/ TCACTGCAT /Zen/

GGACGATCTGTTGCT /3IABkFQ. Exon 10: for 5'- GAGGCCTTAGAGTTAAAGGATG and rev: 5'- AGGGAGGTCTGGGTAGA and probe: 5'-/56-FAM/ CCCATGCTA /Zen/ CAGAGGAGTCTGGAGA /3IABkFQ. The *Rosa* locus was used as a control to normalize values obtained for exon 4 and exon 10 of the *Trp53* locus. *Rosa* locus primers used were: for 5'- GCAATACCTTTCTGGGAGTT and rev 5'- GACTGGAGTTGCAGATCAC and probe 5'-/56FAM/ TGCTGCCTC /ZEN/ CTGGCTTCTGA /3IABkFQ.

Viral expression constructs for mutant TRP53. Whole gene synthesis was utilized to generate each mutant *Trp53* gene expression construct (Genscript). The cDNA sequence corresponding to the full-length coding region of the mutant TRP53 protein was used corresponding to the translation of a 390 amino acid residue protein (391 aa for the insG280). The cDNA construct was flanked at the 5' end by restriction site for *BamHI* and the KOZAK sequence (5'-GGATCCACCATG-3') and the 3' end incorporated a double stop codon and *EcoRI* restriction enzyme site (5'-TGATGAGAATTC). The pMIG vector was linearized using *BglII* and *EcoRI* restriction enzymes, allowing the *Trp53* construct to be cloned into the vector using the *BamHI* and *EcoRI* sites. DNA fragments were ligated together using T4 DNA ligase (Promega). Correct plasmid constructs were screened for by diagnostic digest with *EcoRI* and *XhoI*. Correct construct sequences were subsequently confirmed by standard Sanger sequencing (Australian Genome Research Facility- AGRF, Parkville, Victoria).

sgRNA lentiviral constructs. The inducible lentiviral platform for CRISPR/Cas9 gene modification using dox-inducible sgRNA expression and stable, constitutive expression of CAS9 has been previously described (Aubrey et al. 2015). sgRNA sequences targeting exon 4 and exon 5 of the mouse *Trp53* gene have been previously described (Aubrey et al. 2015).

Oligonucleotides for sgRNA sequences were synthesized (Geneworks, Australia or IDT) and cloned into the pFH1tUTG vector as previously described (Aubrey et al. 2015).

Cell surface staining, flow cytometric analysis and cell sorting. The following fluorochrome-conjugated antibodies were utilized for detection of the cell surface markers: CD19 (clone ID3), B220 (RA3-6B2), IgM (clone 5.1), IgD (clone 11-26C), CD4 (clone H129), CD8 (clone YTS.169), MAC-1 (clone M1/70) and GR-1 (clone RB6-8C5). To confirm the lymphomas were of donor hematopoietic cell derived origin, staining for Ly5.2 (clone a-5.2) and Ly5.1 (clone a-5.1) was also performed. Antibodies were produced and conjugated to R-phycoerythrin (R-PE) or allophycocyanin (APC) in our laboratory.

Intra-cellular flow cytometric analysis of TRP53 protein expression. Cells were first fixed and permeabilized using the BD Fixation and Permeabilization Solutions (Cat#554722). Followed by staining for TRP53 protein using antibody used mouse monoclonal antibody Cell Signaling Clone 1C12 conjugated to AF-647 and fluorescence assessed by flow cytometry using the LSR IIC flow cytometer (Becton Dickinson).

Immunohistochemistry. Antibodies used include TRP53 antibody (anti-TRP53 rabbit polyclonal; Novocastra CM5; 1:500) and the secondary reagent was the DAKO EnVision+ System HRP-conjugated Polymer goat anti-rabbit IgG antibody (Dako K4003). For some tumors arising in the HSPC reconstitution models, additional immunohistochemistry for CD3 (Abcam #ab5690), B220 (RA3-6B2) and F4/80 (F4/80) was performed. Following primary antibody staining, secondary stain was performed using biotinylated goat anti-rabbit Ig (Vector #BA-1000) antibodies or biotin mouse anti-rat IgG2a antibodies (Pharmingen RG7/1.30).

DNA damage analysis. To assess nuclear staining with γ-H2AX, primary B lymphoid cells were first fixed and permeabilized using the BD Fixation and Permeabilization Solutions (Cat#554722). Cells were initially stained with Alexa-Fluor-647 (AF647) conjugated anti-phosphohistone H2A.X (Ser139) ("γ-H2AX") (EMD Millipore Cat#: 05-636-AF647) and subsequently counterstained with DAPI. Slides were then prepared using a Shandon Cytospin centrifuge seeding 30,000 cells per slide. Slides were cover-slipped using Dako fluorescent mounting medium (code S3023). Images were obtained using DeltaVision microscope (GE LIfeScience). Foci measurements were performed in an automated fashion using a custom-written macro in FIJI. Images were processed using a combination of background subtraction, median filtering and auto-thresholding. The cells were segmented from the DAPI channel (to identify nuclei) and the foci were stained with AF647-conjugated antibodies against γ-H2AX, the number and total area of cells and foci were recorded, allowing for a foci area percentage and a number of foci per cell nucleus metric to be calculated.

Tissue culture. *Eμ-Myc* lymphoma-derived cell lines were grown in DME medium supplemented with glucose 4 g/L, 6 mg/mL folic acid, 2 g/L NaHCO3, 116 mg/L L-arginine, 10 mM HEPES, 100 U/mL penicillin and 100 mg/mL streptomycin (Gibco). This DME medium was supplemented with 10% fetal calf serum (FCS) (Gibco or SAFC/Sigma Aldrich), 50 μM mercapto-ethanol (Sigma-Aldrich) and 100 μM asparagine (Sigma-Aldrich) and cells were grown at 37°C in 10% CO_2. Primary B lymphoid cells (for Mitotracker assay) were maintained in Minimum Essential alpha (MEM alpha) medium supplemented with Glutamax (Gibco, 32561-037), 10 mM HEPES (Gibco, 15630-080), 1 mM Sodium pyruvate (Gibco, 11360-070), non-essential amino acid mix to 1X working concentration (Sigma, M7145), 57 μM β-mercapto-ethanol (Sigma, M-6250), 10% FCS and 4% IL-7 (in house production). The primary B lymphoid cells were maintained on the OP9 feeder layer (ATCC CRL-2749) at 37°C

in 10% CO_2. HEK293T cells were maintained in DMEM with 10% FCS (Gibco or SAFC/Sigma Aldrich). Prior to transfection, HEK293T cells were cultured in DME glutamax medium (Gibco) supplemented with 10% FCS and 25 mM Hepes. Primary mouse embryonic fibroblasts were obtained freshly from E13.5 day embryos, from mice of the indicated genotypes, and maintained in DME medium supplemented with 10% fetal calf serum (FCS) (Gibco or SAFC/Sigma Aldrich), 50 μM mercapto-ethanol (Sigma-Aldrich) and 100 μM asparagine (Sigma-Aldrich) and cells were grown at 37°C in 10% CO_2.

RNA-seq analysis. Reads were mapped to the mm10 mouse genome using the Subread aligner (Liao et al. 2013) and assigned to genes using feature Counts (Liao et al. 2014) and Rsubread's built-in refSeq annotation. About 90% of reads were successfully mapped for each sample. Genes that failed to achieve 0.5 counts-per-million (CPM) in at least 2 samples were filtered from the analysis. Immunoglobulin genes and B cell receptor gene segments were removed from the analysis, as were obsolete Entrez gene IDs. Differential gene expression analyses were conducted using the edgeR (McCarthy et al. 2012) and limma (Ritchie et al. 2015) software packages for R. TMM (trimmed mean of M-values) normalization was applied. Multidimensional scaling (MDS) plots were generated with edgeR's plotMDS function. Differential gene expression was assessed using log-linear models and likelihood ratio tests. The three cell lines were included as an additive blocking factor in the linear models so that results were adjusted for baseline differences between the cell lines. The negative binomial dispersions were estimated by edgeR's estimateDisp function (Chen et al. 2014) with robust estimation of the empirical Bayes hyperparameters (Phipson et al. 2016). Tests were conducted to find differentially expressed genes in response to nutlin-3a treatment for each of the mutant TRP53 expressing cells and for the empty-vector pMIG control cells ("treatment effects"). A contrast test was conducted to find genes that were differentially expressed on average in the

mutant TRP53 expressing cells compared to the pMIG vector transduced control cells after nultin-3a treatment ("mutant TRP53 effect"). Gene set tests were performed using edgeR's fry function, which uses a fast approximation to rotation gene set testing (Wu et al. 2010). KEGG pathway analysis used edgeR's kegga function. The list of wt TRP53 target genes was assembled from published TRP53 ChIP-seq and gene expression studies as well as meta-analyses of TRP53 target genes (Riley et al. 2008; Li et al. 2012; Allen et al. 2014), and a list is provided in Supplementary Table 3.

Supplemental Figures with Legends

Supplemental Figure S1. Assessment of mutant TRP53 expression constructs and HSPC reconstitution experiments. (*A*) Retroviral expression construct for each mutant *Trp53* gene with internal ribosomal entry site (IRES) allowing eGFP marker expression. (*B*) Confirmation of high level expression of each mutant TRP53 protein using the retroviral vector in an *Eμ-Myc*;*Trp53*$^{-/-}$ lymphoma cell line, assessed by Western blot analysis with probing for HSP70 used as a loading control. (*C*) BN-PAGE for all five mutant TRP53 proteins in an *Eμ-Myc*;*Trp53*$^{-/-}$ lymphoma cell line to confirm their ability to form multimeric complexes. The less common *Trp53* mutations (V170M, I192S and G280) were compared to the well-characterized TRP53 hot-spot mutants (R246Q and R270H). There is an absence of high molecular weight aggregates as would be seen for mutant TRP53 proteins resulting in conformational changes. (*D*) Representative example of TRP53 protein IHC performed on lymphomas from the *Trp53*$^{-/-}$ HSPC reconstitution experiments. Only 7.5% (3/40) lymphomas expressed the mutant TRP53 protein. (*E*) Representative example of TRP53 protein IHC on lymphomas from the *Trp53*$^{+/-}$ HSPC reconstitution experiments showing heterogeneous pattern of mutant TRP53 staining. (*F*) Representative example of flow cytometric immuno-phenotyping showing an eGFP positive (i.e. mutant TRP53 vector containing), myeloid tumor with expression of the cell surface markers MAC-1 and GR-1, obtained from the *Trp53*$^{+/-}$ HSPC reconstitution experiments. *(G)* Summary of tumor immunophenotyping from the *Trp53*$^{-/-}$ and *Trp53*$^{+/-}$ HSPC reconstitution experiments according to *Trp53* mutation.

Supplement Figure 1

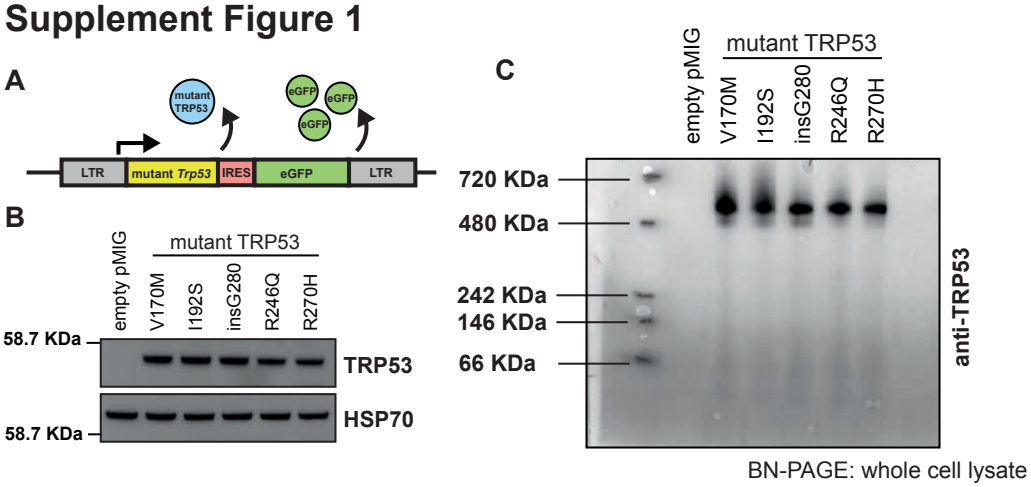

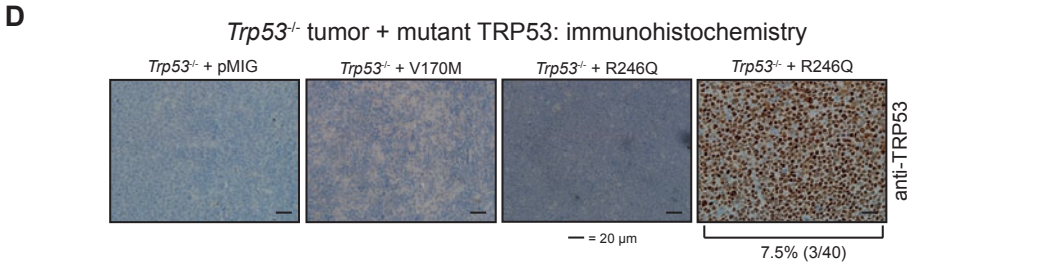

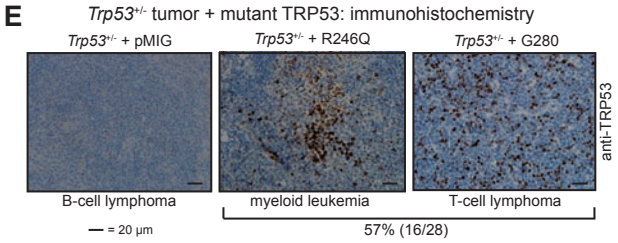

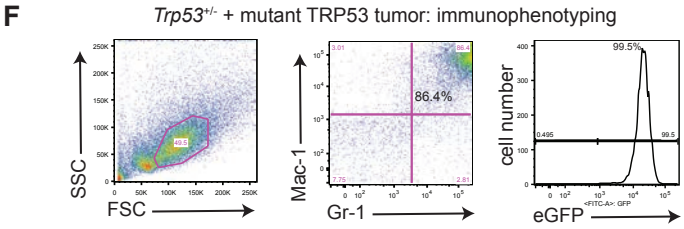

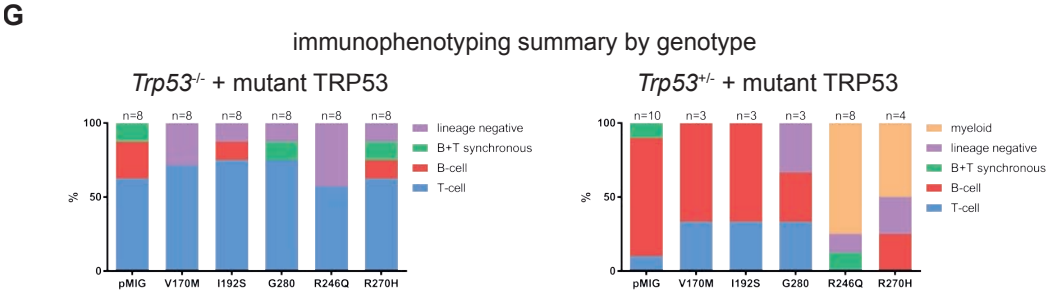

Supplemental Figure S2. Analysis of mutant TRP53-driven *Eμ-Myc* lymphomas. (*A*) Summary of immuno-phenotyping results for surface immunoglobulin expression in mutant TRP53-driven *Eμ-Myc* lymphomas. (*B*) TRP53 protein immuno-histochemistry. R246Q and R270H TRP53 mutant proteins are uniformly associated with low-level, heterogeneous, nuclear mutant TRP53 protein expression in the lymphomas. Mouse numbers (bottom right) and scale bars are indicated in each panel. The lymphoma in the control mouse #75 exhibited a spontaneous endogenous *Trp53* mutation confirmed by sequencing. An additional lymphoma that had acquired a spontaneous R270H mutation in the endogenous *Trp53* allele was included as an additional control. (*C*) Summary analysis of early passage lymphoma-derived cell lines for sensitivity to etoposide. Data represent mean+/-SEM with p-value by paired t-test (*$p<0.05$). (*D*) Analysis of gene expression for selected *Trp53* target genes 6 h after treatment with 10μM nutlin-3a of selected cell lines derived from the tumors depicted in Fig. 2C and Supplemental Fig. S2C.

Supplement Figure 2

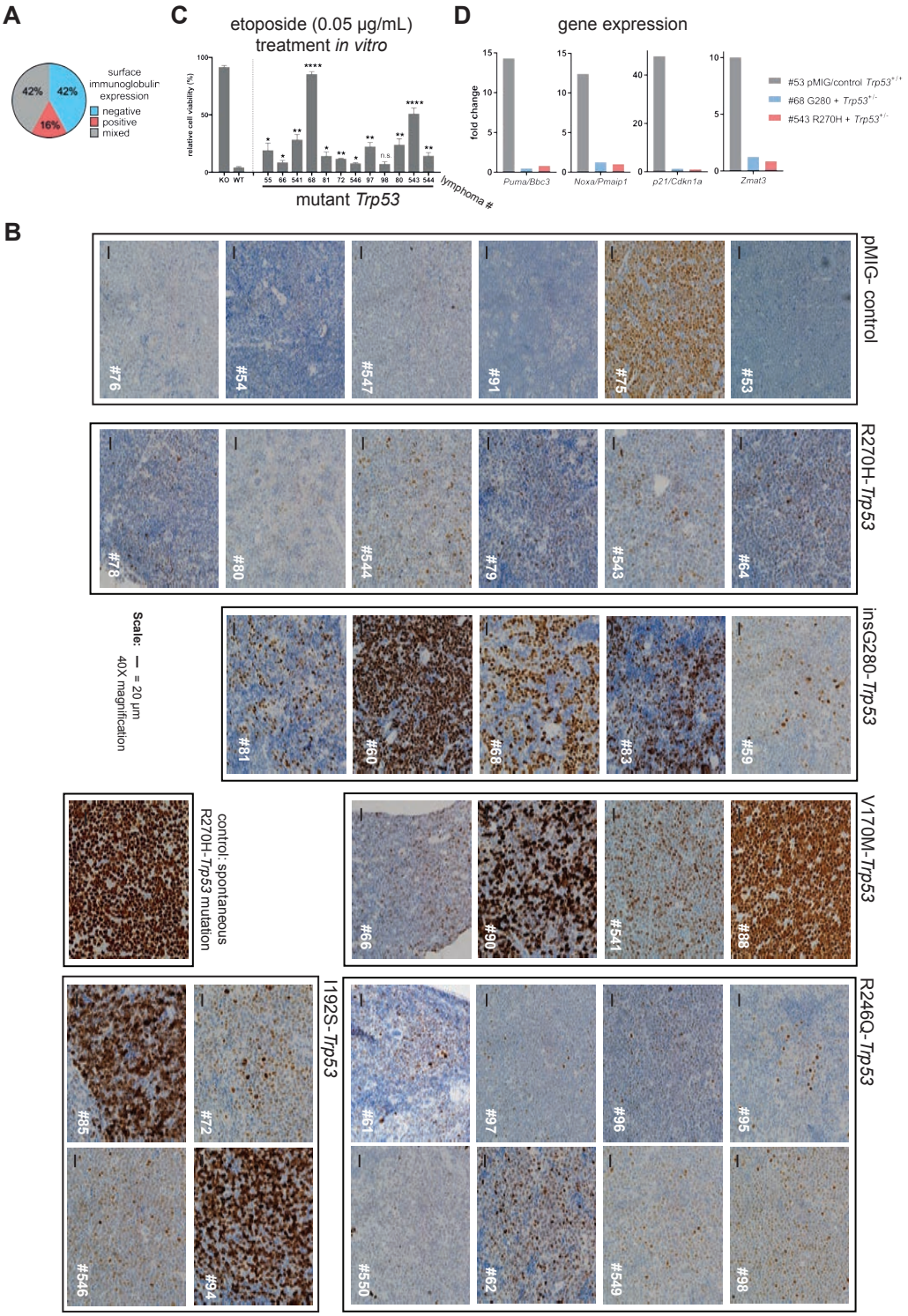

Supplemental Figure S3. Protein stability and impact on gene expression of TRP53 mutants. (*A*) Western blot analysis for the indicated TRP53 (mutant and wt) proteins and p19/ARF protein, with HSP70 used as loading control, with and without CRISPR/Cas9 mediated inactivation of the endogenous wt *Trp53* gene, and with or without treatment with nutlin-3a. (*B*) Western blot analysis of primary mouse embryonic fibroblasts (genotypes $Trp53^{+/+}$, $Trp53^{+/-}$ and $Trp53^{-/-}$) for TRP53 and P19/ARF proteins with exogenous over-expression of R246Q and R270H mutant TRP53, with HSP70 used as loading control. (*C*) Multi-dimensional scaling (MDS) plots showing overall differences between the RNA-seq expression profiles. The same plot is shown with three keys corresponding to (i) treatment, (ii) cell line and (iii) *Trp53* mutation. Panel (ii) shows that the *Eμ-Myc* lymphoma cell lines (287, 621 and AF47A) have distinct gene expression profiles and that the nutlin-3a treatment has a strong effect for each cell line. Panel (iii) shows more subtle differences between the five distinct *Trp53* mutations. Distances on the plots represent leading log-fold change, which is the root mean square average of the largest 500 expression log-2 fold changes between each pair of samples. (*D*) RNA-seq expression values (log-2 counts per million) for *Trp53, Puma/Bbc3*, and *Noxa/Pmaip1* mRNAs. Expression values are averaged over the 3 cell lines for each TRP53 mutant. The five *Trp53* mutants have similar mRNA expression levels and show an average log-2 fold change of 2.32 compared to pMIG transduced control cells with the DMSO treatment (FDR < 1e-25). (*E*) Time course qRT-PCR at 6, 12 and 24 h of treatment with nutlin-3a (5 μM). Single *Eμ-Myc* cell line transduced with an expression construct for R270H mutant TRP53 protein. Different wt TRP53 target genes show variable repression of nutlin-3a-induced gene expression induction by the mutant TRP53 proteins. The greatest variability occurred at the 6 h time point with *Zmat3* remaining not affected (red arrow) while other targets (e.g. *Ercc5*) were already strongly repressed. At later time points, a more global DNE was evident. *Rock1* expression was not significantly different in the presence of mutant TRP53 compared

to control cells. Data represent mean+/-SEM for n=3 independent experiments. p-value for pMIG control *vs* mutant TRP53 determined by 2-way ANOVA.

Supplement Figure 3

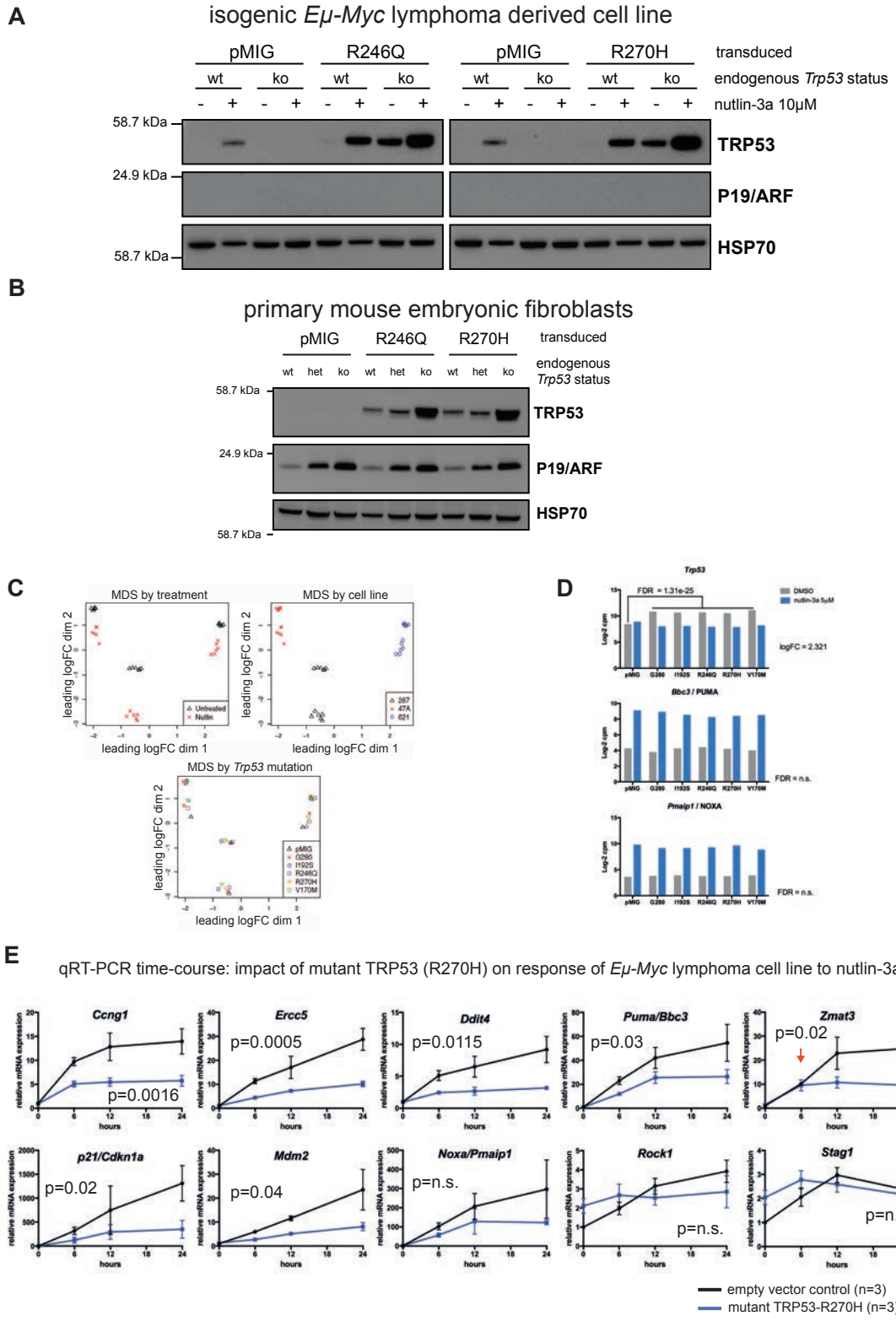

Supplemental Figure S4. Analysis of pre-leukemic hot-spot mutant TRP53-transduced pre-leukemic *Eμ-Myc* B-lymphoid cells in reconstituted mice. (*A*) Peripheral blood lymphocyte counts and organ weights (lymph nodes, spleen, thymus) at the 4-week time point of analysis in lethally irradiated mice reconstituted with HSPCs from the fetal liver of *Eμ-Myc* mice that had been transduced with mutant TRP53 expression vectors or a control vector. Data represent mean+/-SEM. (*B*) Summary of hot-spot mutant TRP53 expression vector (N= 2 different TRP53 mutants) or control vector transduction efficiency at the time of analysis, as indicated by eGFP expression in pre-leukemic *Eμ-Myc* B lymphoid cells from the bone marrow of HSPC reconstituted mice (n=number of recipient mice examined). Data represent mean+/-SEM. (*C,D*) Survival of pre-leukemic *Eμ-Myc* B lymphoid cells (CD19+B220+GFP+) with the hot-spot mutant TRP53 expression vectors (N= 2 different TRP53 mutants) or the control vector in (*C*) serum containing or (*D*) serum-free culture medium, both not supplemented with extra cytokines (e.g. IL-7). (n=number of recipient mice examined). Data represent mean+/-SEM. (*E*) DNA damage assessment in pre-leukemic *Eμ-Myc* B lymphoid cells (B220+CD19+GFP+) with the indicated mutant TRP53 expression vectors or the control vector in the basal state by using the comet assay, indicating increased DNA damage by trend toward longer comet tail moment. For each sample 100-250 comet tails were measured. Data represent mean+/-SEM; pMIG control n=4, R246Q n=5, R270H n=5. Images depict representative examples of comet tails obtained for pre-leukemic *Eμ-Myc* B lymphoid cells (B220+CD19+) expressing the R246Q or R270H TRP53 mutant proteins as compared to the empty vector/pMIG control transduced cells are shown. (*F*) Hematoxylin and eosin (H&E) stain and immunohistochemistry for mutant TRP53 protein on sections of bone marrow and thymus from mice reconstituted with *Eμ-Myc* transgenic HSPCs that had been transduced with either empty vector control (pMIG) or mutant TRP53 (R246Q or R270H) expression vectors. (*G*) Efficient transduction with the mutant TRP53 expression vector of bone marrow derived pre-leukemic

Eμ-Myc B lymphoid cells in HSPC reconstituted mice (as depicted in *F*) by assessment of eGFP expression by flow cytometry (representative example). (*H*) Mutant TRP53 protein levels in pre-leukemic mutant TRP53 vector transduced pre-leukemic *Eμ-Myc* B lymphoid cells from HSPC reconstituted mice as assessed by intra-cellular FACS. Data represent mean+/-SEM; pMIG control (blue) n=4, mutant TRP53 (red) n=3 for R246Q and n=4 for R270H (these data were combined), control *Eμ-Myc* lymphoma line #412 that has a spontaneous R246Q TRP53 mutation (green) n=1.

Supplement Figure 4

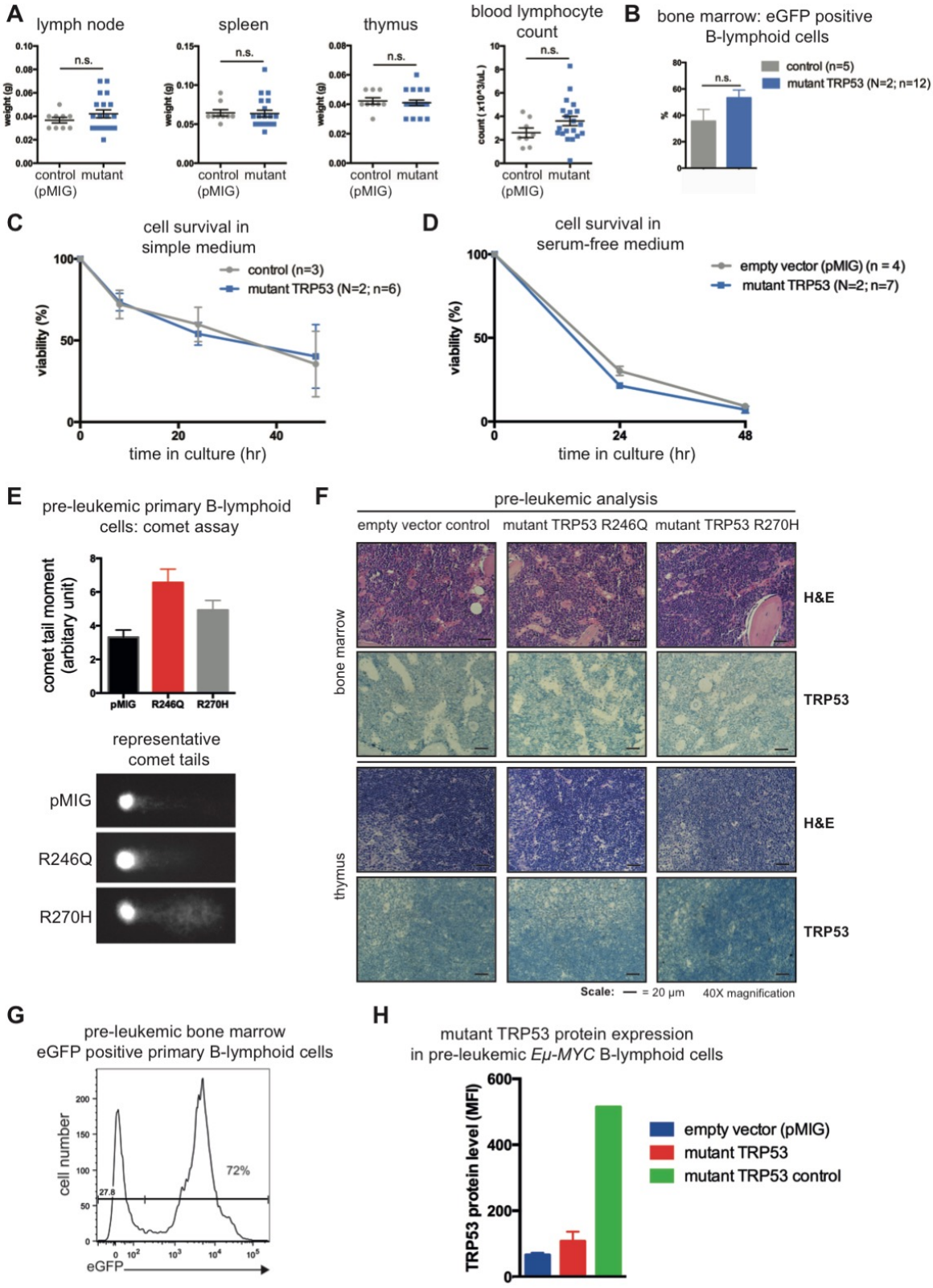

Supplemental Figure S5. Transcriptional analysis of the DNE of mutant TRP53 in pre-leukemic mutant TRP53-transduced *Eμ-Myc* B-lymphoid cells in reconstituted mice and comparison to nutlin-3a treated established *Eμ-Myc* lymphoma-derived cell lines. (*A*) RNA-seq analysis barcode plots for TRP53 gene set test in the nutlin-3a-treated state in *Eμ-Myc* lymphoma-derived cell lines transduced with each mutant TRP53 construct. N=5 mutant TRP53 proteins in n=3 biological replicates for each cell line; for pMIG control, n=3 biological replicates for each cell line. (*B*) RNA-seq analysis barcode plots for TRP53 gene set test in the steady-state (no treatment with nutlin-3a; directly *ex vivo*) in pre-leukemic *Eμ-Myc* transgenic B lymphoid cells transduced with the indicated mutant TRP53 constructs. N=5 mutant TRP53 proteins in n=3 biological replicates each; for pMIG control, n=3 pre-leukemic samples. (p-values by FRY test, restricted to TRP53 gene set).

Supplemental Figure S5

A *Eμ-Myc* lymphoma cell lines in nutlin-3a-treated state

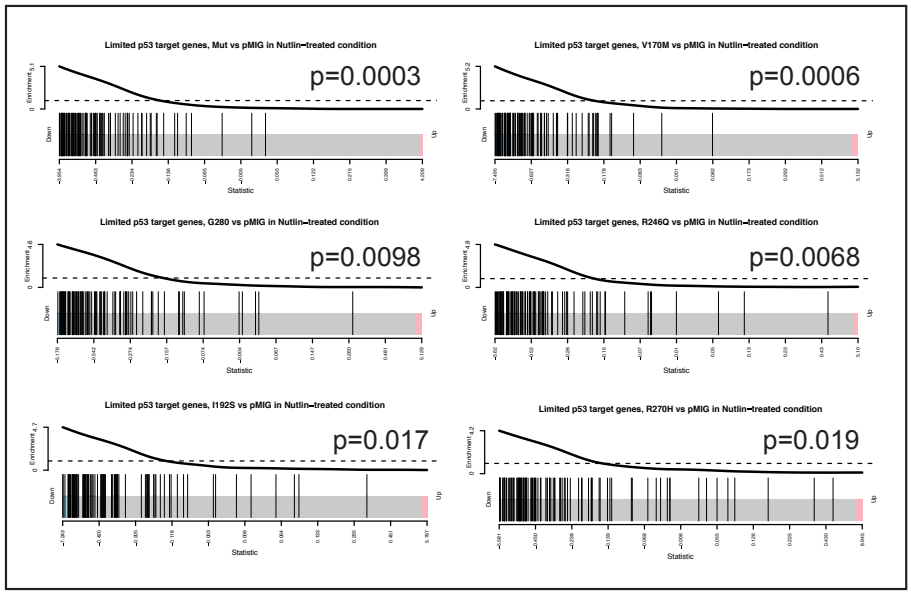

B pre-leukemic *Eμ-Myc* B lymphoid cells in steady state

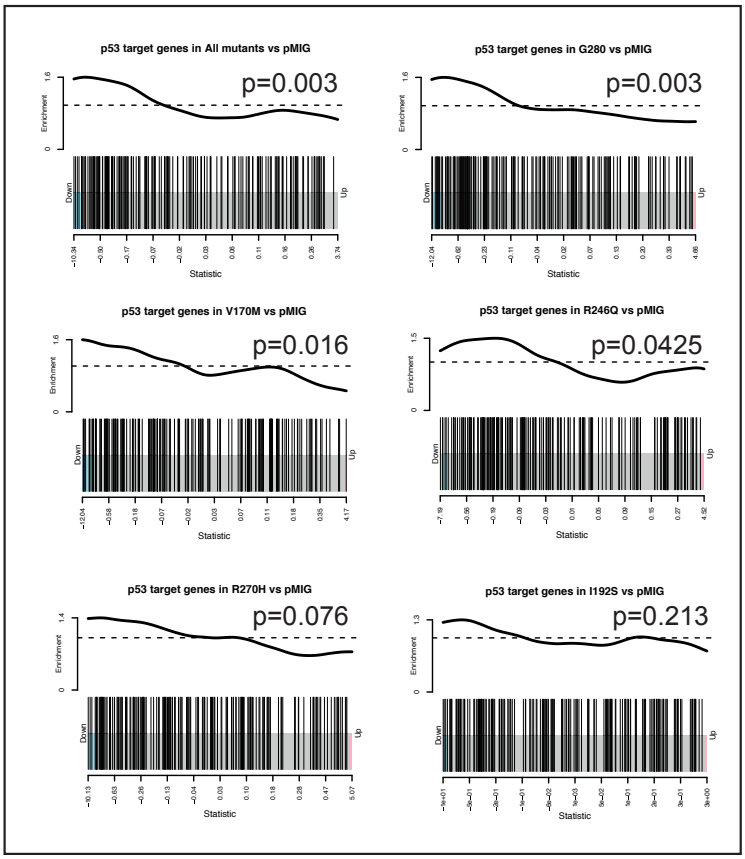

Supplemental Table S1. RNA-seq data: list of differentially expressed genes in the empty vector (pMIG)-transduced control *Eμ-Myc* lymphoma cell lines (n=3 biological replicates) after treatment with nutlin-3a. Columns show Entrez Gene ID, gene symbol, log2 fold change, average log2 counts per million, chi-square likelihood ratio test, p-value and false discovery rate.

Supplemental Table S2. RNA-seq data: list of differentially expressed genes between the average of the five mutant TRP53-transduced cell lines (N=5 mutant TRP53 proteins in n=3 biological replicates each) and the empty vector (pMIG)-transduced control *Eμ-Myc* lymphoma cell lines after treatment with nutlin-3a (n=3 biological replicates). Columns are as for Supplemental Table 1.

Supplemental Table S3. List of wt TRP53 target genes used for the RNA-seq wt TRP53 target gene set test analyses in Figure 3.

Supplemental Table S4. RNA-seq data: wt TRP53 target gene set analysis. Analyses were performed on the entire gene set (ROAST test) as well as restricting the set to those genes that were significantly induced in empty vector (pMIG)-transduced control *Eμ-Myc* lymphoma cell lines after treatment with nutlin-3a (to visualize in the heat map) (Figure 3F). Differentially expressed genes between mutant TRP53-transduced *Eμ-Myc* lymphoma cell lines (N=5 mutant TRP53 proteins in n=3 different cell lines) and empty vector (pMIG)-transduced control *Eμ-Myc* lymphoma cell lines after treatment with nutlin-3a were identified and additional mutant TRP53-specific analysis was performed on nutlin-3a treatment induced genes only.

Supplemental Table S5. Kyoto Encyclopedia of Genes and Genomes (KEGG) pathway analysis of differentially expressed genes between mutant TRP53-transduced *Eμ-Myc* lymphoma cell lines and empty vector (pMIG)-transduced control *Eμ-Myc* lymphoma cell lines after treatment with nutlin-3a. Columns show pathway ID, pathway name, number of genes in the pathway (N), number of genes in the pathway that are up-regulated (FDR < 0.05), number of genes in the pathway that are down-regulated (FDR < 0.05), p-value for up-regulated and p-value for down-regulation.

Supplemental Table S6. RNA-seq data from pre-leukemic *Eμ-Myc* B lymphoid cell set: differentially expressed genes between the average of the five mutant TRP53-transduced pre-leukemic B lymphoid cells (N=5 mutant TRP53 proteins in n=3 biological replicates each) and the empty vector (pMIG)-transduced control pre-leukemic cells at steady state directly *ex vivo* (no treatment with nutlin-3a). Columns are as for Supplemental Table 1.

Author Contributions

B.J.A., G.L.K and A.S. wrote the manuscript. B.J.A, G.L.K and A.S. conceptualized and planned the study. A.K.V. performed data analysis. Y.C. and G.K.S performed bioinformatics analysis and contributed to writing the manuscript. L.W. assisted with confocal microscopy and performed automated image analysis. A.J.K., G.D., and L.O.R. provided valuable advice and important reagents. B.J.A., A.J., C.C., E.C.L., S.T.D., J.P.B., A.S. and G.L.K performed experiments and analyzed data.

References

Allen MA, Andrysik Z, Dengler VL, Mellert HS, Guarnieri A, Freeman JA, Sullivan KD, Galbraith MD, Luo X, Kraus WL et al. 2014. Global analysis of p53-regulated transcription identifies its direct targets and unexpected regulatory mechanisms. *Elife* **3**: e02200.

Aubrey BJ, Kelly GL, Kueh AJ, Brennan MS, O'Connor L, Milla L, Wilcox S, Tai L, Strasser A, Herold MJ. 2015. An inducible lentiviral guide RNA platform enables the identification of tumor-essential genes and tumor-promoting mutations in vivo. *Cell reports* **10**: 1422-1432.

Chen Y, Lun ATL, Smyth GK. 2014. Differential expression analysis of complex RNA-seq experiments using edgeR. in *Statistical Analysis of Next Generation Sequence Data* (eds. S Datta, DS Nettleton), pp. 51-74. Springer, New York.

Li M, He Y, Dubois W, Wu X, Shi J, Huang J. 2012. Distinct regulatory mechanisms and functions for p53-activated and p53-repressed DNA damage response genes in embryonic stem cells. *Mol Cell* **46**: 30-42.

Liao Y, Smyth GK, Shi W. 2013. The Subread aligner: fast, accurate and scalable read mapping by seed-and-vote. *Nucleic Acids Res* **41**: e108.

-. 2014. featureCounts: an efficient general purpose program for assigning sequence reads to genomic features. *Bioinformatics* **30**: 923-930.

McCarthy DJ, Chen Y, Smyth GK. 2012. Differential expression analysis of multifactor RNA-Seq experiments with respect to biological variation. *Nucleic Acids Res* **40**: 4288-4297.

Phipson B, Lee S, Majewski IJ, Alexander WS, Smyth GK. 2016. Robust Hyperparameter Estimation Protects against Hypervariable Genes and Improves Power to Detect Differential Expression. *The annals of applied statistics* **10**: 946-963.

Riley T, Sontag E, Chen P, Levine A. 2008. Transcriptional control of human p53-regulated genes. *Nat Rev Mol Cell Biol* **9**: 402-412.

Ritchie ME, Phipson B, Wu D, Hu Y, Law CW, Shi W, Smyth GK. 2015. limma powers differential expression analyses for RNA-sequencing and microarray studies. *Nucleic Acids Res* **43**: e47.

Wu D, Lim E, Vaillant F, Asselin-Labat ML, Visvader JE, Smyth GK. 2010. ROAST: rotation gene set tests for complex microarray experiments. *Bioinformatics* **26**: 2176-2182.